Journal of Materials Chemistry A

COMMUNICATION

View Article Online
View Journal | View Issue

Cite this: J. Mater. Chem. A, 2015, 3, 4799

Received 13th November 2014
Accepted 26th January 2015

DOI: 10.1039/c4ta06142j

www.rsc.org/MaterialsA

Hierarchically micro/mesoporous activated graphene with a large surface area for high sulfur loading in Li–S batteries†

Ya You,[a] Wencong Zeng,[b] Ya-Xia Yin,[a] Juan Zhang,[a] Chun-Peng Yang,[a] Yanwu Zhu*[b] and Yu-Guo Guo*[a]

A hierarchically micro/mesoporous a-MEGO with a high surface area (up to 3000 $m^2 g^{-1}$) and large pore volume (up to 2.14 $cm^3 g^{-1}$) was utilized as a superior carbon host material for high sulfur loading towards advanced Li–S batteries.

Motivated by the increasing demand of advanced energy storage systems, lithium–sulfur (Li–S) batteries are considered as promising candidates for the next generation of high-energy storage devices due to their high theoretical specific capacity (1675 mA h g^{-1}) and energy density (~2600 W h kg^{-1}).[1–9] However, the application of Li–S batteries is still inhibited by various problems, which mostly originate from the sulfur cathode. On one hand, sulfur exhibits poor ionic and electronic conductivities, leading to a relatively high resistance.[10] On the other hand, the highly electrolyte-soluble polysulfide intermediates will give rise to a loss of active materials and a shuttle effect, responsible for the rapidly fading capacity and poor Coulombic efficiency.[11–18]

One of the most effective ways to enhance the performance of the sulfur cathode is by impregnating sulfur into various conducting substrates,[19,20] such as carbon nanotubes (CNTs),[21] graphene,[22] porous carbon,[23] and conductive polymers.[24,25] The loading of sulfur in these substrates is a very important issue. Since the substrate contributes negligible capacities between the working voltage ranges of Li–S batteries, a low sulfur loading would lead to a reduced overall volumetric capacity and energy density of the cathode.[26] Nevertheless, achieving high sulfur loading (>70 wt%) is a big challenge because the S/C composite cathode may show a poor electrochemical activity due to the intrinsic electronic insulation of sulfur.[27] Besides, a high sulfur content would also lead to a severe dissolution of polysulfides and shuttle effect.

Graphene, a single-atom-thick carbon material, has been utilized as a substrate for sulfur loading because of its extremely high conductivity, flexibility, and a high theoretical specific surface area (SSA) of 2600 $m^2 g^{-1}$.[28–30] However, due to the agglomeration of the graphene sheets, it exhibits a much lower SSA than the theoretical value, leading to relatively low sulfur loading. What is more, since graphene is a two dimensional (2D) material, sulfur only infiltrates onto the surface or the pores formed by the crumpled graphene sheets, which is hard to alleviate the dissolution of polysulfides into the electrolyte.[31,32] Many efforts have been devoted to improve the performance of the graphene/S cathode, such as surface coating by conductive polymers[33] and reduced graphene oxides,[34] heteroatom doping,[35] surface hydroxyl modification[36] and constructing three dimensional (3D) graphene conductive networks.[37] Recently, constructing porous graphene has aroused great attention. Zhang's group[38] demonstrated a mesoporous graphene with a pore size of ~3.8 nm produced by activating hydrothermally reduced graphene oxide hydrogels for 60 wt% sulfur loading. The S/C composite exhibited a high capacity up to 1379 mA h g_{sulfur}^{-1} at 0.2 C, however, the cycling performance was limited within 60 cycles since the sole use of mesoporous carbon cannot completely suppress the dissolution of polysulfides. Micropores have been proved to effectively confine polysulfides.[39] However, it also suffers from a low energy density (<50 wt% sulfur) and a sluggish Li^+ diffusion process.[40] Recently, carbon hosts with micro/mesoporous structure have been considered as ideal substrates to achieve the balance between sulfur confinement and loading.[41]

Herein, a hierarchically micro/mesoporous activated graphene (a-MEGO) with high SSA was utilized in Li–S batteries. Employing microwave exfoliated graphene oxide (MEGO) as a precursor, a-MEGO exhibits a high SSA of up to 3000 $m^2 g^{-1}$ exceeding the theoretical value of graphene, a high pore volume

[a]CAS Key Laboratory of Molecular Nanostructure and Nanotechnology, Beijing National Laboratory for Molecular Sciences, Institute of Chemistry, Chinese Academy of Sciences (CAS), Beijing 100190, P. R. China. E-mail: ygguo@iccas.ac.cn; Fax: +86-10-82617069; Tel: +86-10-82617069

[b]Department of Materials Science and Engineering, CAS Key Laboratory of Materials for Energy Conversion, University of Science and Technology of China, Hefei 230026, P. R. China. E-mail: zhuyanwu@ustc.edu.cn; Fax: +86-551-63601696; Tel: +86-551-63607670

† Electronic supplementary information (ESI) available: Experimental section and additional data on the a-MEGO/S composite. See DOI: 10.1039/c4ta06142j

of 2.14 cm^3 g^{-1}, a 3D carbon conductive network, and a hierarchically micro/mesoporous structure (0.6–5 nm).[42] Due to the extremely high SSA and pore volume, a-MEGO could achieve a high sulfur loading of 75 wt%, leading to a high overall energy density. Meanwhile, the hierarchically micro/mesoporous structure could ensure an effective confinement of polysulfide. As a result, the composite exhibits a high specific capacity of 789 mA h g^{-1} (based on the composite) at 0.15 C with a Coulombic efficiency of ~100%. The capacity retention of a-MEGO/S could reach 76% after 200 cycles at 1 C.

The preparation route of the a-MEGO/S composite is shown in Fig. 1. To begin with, MEGO was prepared by exfoliating graphene oxide (GO) in a microwave oven.[43] Then MEGO went through a KOH activation process to yield a-MEGO (Fig. 1a and b).[42] According to the X-ray diffraction (XRD) patterns (see Fig. S1, ESI†), the sharp peak of GO at around 10° disappeared after microwave irradiation and KOH activation process, demonstrating full exfoliation of GO into graphene sheets. The obtained a-MEGO shows 3D bulk morphology (see Fig. S2a and b, ESI†), which is quite different from the typical thermal reduced graphene oxide.[34] This 3D carbon framework could provide effective pathways for electron transportation. Sulfur was introduced to form the a-MEGO/S composite through a vapor phase infusion method to facilitate the infusion of sulfur into the carbon matrix[44] (Fig. 1c). After heat treatment, the characteristic XRD peaks of orthorhombic S (JCPSD no. 08-0247) and Raman vibration peaks of α-S_8 have disappeared (Fig. S3, see ESI†), demonstrating that sulfur exists as amorphous type and is finely incorporated into the nanopores of a-MEGO. Consistently, no sulfur particles are observed on the surface of a-MEGO (Fig. 2a and b), indicating good incorporation of sulfur into the a-MEGO substrate. In the high resolution transmission electron microscopy (HRTEM) image of the a-MEGO/S composite (Fig. 2c), no crystalline sulfur spacing can be observed, which is in good agreement with the XRD results. Scanning transmission electron microscopy (STEM) and elemental mapping analysis with good match between the sulfur (yellow) and the carbon (red) maps further confirm that the sulfur elements distribute homogeneously among the carbon substrates (Fig. 2d–f).

N_2 adsorption/desorption isotherms were employed to investigate the pore structures of a-MEGO and a-MEGO/S composites (see Fig. S4, ESI†). The results show that a-MEGO has a large Brunauer–Emmett–Teller (BET) SSA of 2994.8 m^2 g^{-1}.[42] After sulfur impregnation, the SSA of the a-MEGO/S composite is as low as 0.066 m^2 g^{-1}, indicating well incorporation of

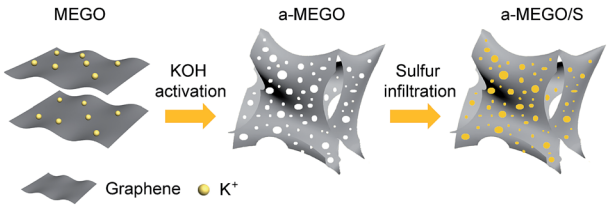

Fig. 1 Schematic illustration of the preparation of the a-MEGO/S composite.

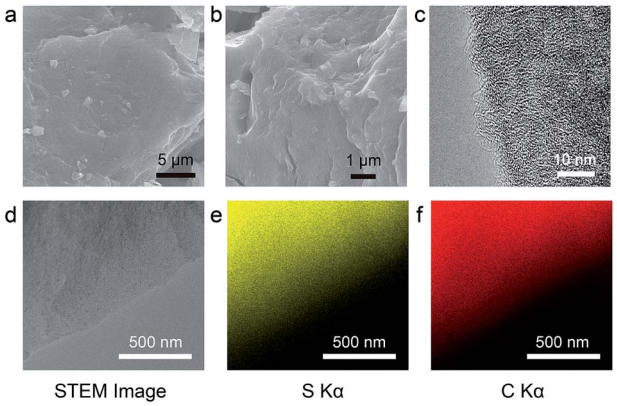

Fig. 2 (a and b) SEM images, (c) HETEM image, (d) bright field STEM image and the corresponding (e) S and (f) C EDX elemental mappings of the a-MEGO/S composite.

sulfur. According to the high pore volume (up to 2.14 cm^3 g^{-1}), a-MEGO could contain 81 wt% sulphur theoretically, and the actual sulfur content is demonstrated as high as 75 wt% as shown in thermogravimetric analysis (TGA) in Fig. S5 (see ESI†). This sulfur loading is much higher than many reported values, *e.g.*, 50 wt% for hydroxylated graphene[36] and 47 wt% for polyacrylonitrile/graphene.[45] Due to the high SSA and a continuous 3D network of pores, high sulfur loading with homogeneous distribution was achieved.

Cycle voltammograms (CV) of a-MEGO/S cathode are shown in Fig. 3a. Since a-MEGO shows the presence of micropores mainly in the ~1 nm size range with a very small proportion of pores less than 0.5 nm, which means most of the sulfur in the a-MEGO/S composite is cyclo-S_8, typical output voltages of Li–S

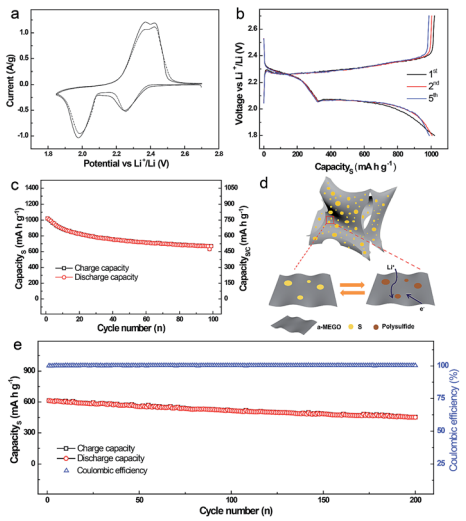

Fig. 3 (a) Cyclic voltammograms of the a-MEGO/S at a scanning rate of 0.1 mV s^{-1}. The solid and dashed line correspond to the first and second cycle, respectively. (b) Galvanostatic charge/discharge voltage profiles and (c) cycling performance of the a-MEGO/S at 0.15 C. (d) A scheme of the electrochemical reaction process of the a-MEGO/S composite for its improved electrochemical performance. (e) Cycling performance of the a-MEGO/S at 1 C.

batteries with two reduction peaks at 2.25 and 2.0 V were observed.[39,46] There are only slight changes of the CV peak positions in the second cycle, demonstrating a good electrochemical reversibility. For the a-MEGO/S composite, the initial discharge capacity is as high as 765 mA h g^{-1} (1020 mA h g^{-1} based on the mass of sulfur), with a high initial Coulombic efficiency of ~100% (Fig. 3b). When calculated on the mass of the whole composite, the capacity is much better than many reported S/C composites with low sulfur contents, which shows high specific capacity on sulfur but low capacity on the composite.[47] Due to the high conductivity and 3D electron transporting pathways, the a-MEGO/S also exhibits good rate capabilities (see Fig. S6, ESI†). When cycled at 1 C, the capacity retention could be 71.2% compared with that at 0.2 C. After 100 cycles, the a-MEGO/S could deliver a capacity of 502 mA h g^{-1}, (670 mA h g^{-1} based on the mass of sulfur) at 0.15 C (Fig. 3c). The cycling performance and the corresponding Coulombic efficiencies of a-MEGO/S with a high current density of 1 C are shown in Fig. 3e. The capacity retention could reach 76% after 200 cycles. The Coulombic efficiencies always are 100%, even under low current densities, demonstrating that the a-MEGO could effectively diminish the shuttle effects of polysulfides. After 200 cycles at 1 C, the a-MEGO/S cathode could still maintain a homogeneous distribution of sulfur in the a-MEGO matrix in view of the good match between sulfur and carbon maps (see Fig. S7, ESI†), indicating a superior cycling stability. The enhanced performance is attributed to the hierarchically micro/mesoporous structure, which could effectively confine polysulfides into the nanopores and prevent them from dissolving into the electrolyte (Fig. 3d).

The improved electrochemical performance of a-MEGO/S might originate from the following aspects. (1) The extremely high SSA exceeding the theoretical value of graphene and a high pore volume promise a high sulfur loading, further leading to an increased energy density and volume density of the cathode. (2) The micropores and mesopores of a-MEGO could function as reservoirs for polysulfide and play an important role in absorbing and confining polysulfides, which result in a suppressed shuttle effect, improved Coulombic efficiency and cycling stability eventually. (3) The 3D carbon frameworks and the inter-connected pores ensure effective pathways for fast ion diffusion and electron transportation, proving a good rate capability.

In summary, a micro/mesoporous a-MEGO with a high SSA of ~3000 m^2 g^{-1} and a large pore volume of ~2.14 cm^3 g^{-1} was utilized as a carbon substrate for high sulfur loading in Li–S batteries. Due to the high SSA and the porous structure, the a-MEGO could ensure a homogeneous distribution of sulfur even at a high sulfur loading of 75 wt%. When applied as a cathode in Li–S batteries, the a-MEGO/S exhibits high specific capacity, good rate capabilities and impressive cycling stability. The good electrochemical performance of a-MEGO/S could be attributed to its unique 3D hierarchically micro/mesoporous structure, which could function as superior reservoirs for polysulfides and suppress their diffusion into the electrolyte. The results demonstrate that a-MEGO is a promising host material to realize high sulfur loading as well as superior electrochemical performance at the same time for advanced Li–S batteries with high energy density, high rate capability and long cycle life. In view of the electrochemistry similarity between elemental sulphur and selenium, the a-MEGO may also be extended to Li–Se batteries.[48]

Acknowledgements

This work was supported by the National Natural Science Foundation of China (Grants 51225204, 51322204, and U1301244), the National Basic Research Program of China (Grants 2011CB935700 and 2012CB932900), the "Strategic Priority Research Program" of the Chinese Academy of Sciences (Grant XDA09010300), and the Fundamental Research Funds for the Central Universities (WK2060140014).

Notes and references

1 L. Peng, X. Peng, B. Liu, C. Wu, Y. Xie and G. Yu, *Nano Lett.*, 2013, **13**, 2151.
2 L. Suo, Y.-S. Hu, H. Li, M. Armand and L. Chen, *Nat. Commun.*, 2013, **4**, 1481.
3 J. Guo and C. Wang, *Chem. Commun.*, 2010, **46**, 1428.
4 J. Zhou, Q. Liang, A. Pan, X. Zhang, Q. Zhu, S. Liang and G. Cao, *J. Mater. Chem. A*, 2014, **2**, 11029.
5 W. Guo, Y.-X. Yin, S. Xin, Y.-G. Guo and L.-J. Wan, *Energy Environ. Sci.*, 2012, **5**, 5221.
6 Y.-X. Yin, S. Xin, Y.-G. Guo and L.-J. Wan, *Angew. Chem., Int. Ed.*, 2013, **52**, 13186.
7 H.-X. Ji, X.-L. Wu, L.-Z. Fan, C. Krien, I. Fiering, Y.-G. Guo, Y. Mei and O. G. Schmidt, *Adv. Mater.*, 2010, **22**, 4591.
8 P. Han, W. Ma, S. Pang, Q. Kong, J. Yao, C. Bi and G. Cui, *J. Mater. Chem. A*, 2013, **1**, 5949.
9 X. Zhou, A.-M. Cao, L.-J. Wan and Y.-G. Guo, *Nano Res.*, 2012, **5**, 845.
10 N. Jayaprakash, J. Shen, S. S. Moganty, A. Corona and L. A. Archer, *Angew. Chem., Int. Ed.*, 2011, **50**, 5904.
11 H.-J. Peng, J.-Q. Huang, M.-Q. Zhao, Q. Zhang, X.-B. Cheng, X.-Y. Liu, W.-Z. Qian and F. Wei, *Adv. Funct. Mater.*, 2014, **24**, 2772.
12 Y. Fu, Y.-S. Su and A. Manthiram, *Angew. Chem., Int. Ed.*, 2013, **52**, 6930.
13 J. Kim, D.-J. Lee, H.-G. Jung, Y.-K. Sun, J. Hassoun and B. Scrosati, *Adv. Funct. Mater.*, 2013, **23**, 1076.
14 H. Jia, J. Wang, F. Lin, C. W. Monroe, J. Yang and Y. NuLi, *Chem. Commun.*, 2014, **50**, 7011.
15 X.-G. Sun, X. Wang, R. T. Mayes and S. Dai, *ChemSusChem*, 2012, **5**, 2079.
16 C. Huang, J. Xiao, Y. Shao, J. Zheng, W. D. Bennett, D. Lu, L. V. Saraf, M. Engelhard, L. Ji, J. Zhang, X. Li, G. L. Graff and J. Liu, *Nat. Commun.*, 2014, **5**, 3015.
17 N. Li, Z. Weng, Y. Wang, F. Li, H.-M. Cheng and H. Zhou, *Energy Environ. Sci.*, 2014, **7**, 3307.
18 Y. Yan, Y. Yin, Y. Guo and L.-J. Wan, *Sci. China: Chem.*, 2014, **57**, 1564.
19 X. Ji, K. T. Lee and L. F. Nazar, *Nat. Mater.*, 2009, **8**, 500.
20 W. Weng, V. G. Pol and K. Amine, *Adv. Mater.*, 2013, **25**, 1608.

21 Y. Zhao, W. Wu, J. Li, Z. Xu and L. Guan, *Adv. Mater.*, 2014, **26**, 5113.
22 L. Ji, M. Rao, H. Zheng, L. Zhang, Y. Li, W. Duan, J. Guo, E. J. Cairns and Y. Zhang, *J. Am. Chem. Soc.*, 2011, **133**, 18522.
23 K. Zhang, Q. Zhao, Z. Tao and J. Chen, *Nano Res.*, 2013, **6**, 38.
24 G.-C. Li, G.-R. Li, S.-H. Ye and X.-P. Gao, *Adv. Energy Mater.*, 2012, **2**, 1238.
25 G. Ma, Z. Wen, J. Jin, Y. Lu, X. Wu, C. Liu and C. Chen, *RSC Adv.*, 2014, **4**, 21612.
26 G. Zhou, D.-W. Wang, F. Li, P.-X. Hou, L. Yin, C. Liu, G. Q. Lu, I. R. Gentle and H.-M. Cheng, *Energy Environ. Sci.*, 2012, **5**, 8901.
27 Y.-X. Wang, L. Huang, L.-C. Sun, S.-Y. Xie, G.-L. Xu, S.-R. Chen, Y.-F. Xu, J.-T. Li, S.-L. Chou, S.-X. Dou and S.-G. Sun, *J. Mater. Chem.*, 2012, **22**, 4744.
28 S. Evers and L. F. Nazar, *Chem. Commun.*, 2012, **48**, 1233.
29 Y. Zhao, C. Hu, L. Song, L. Wang, G. Shi, L. Dai and L. Qu, *Energy Environ. Sci.*, 2014, **7**, 1913.
30 Z. Xing, B. Wang, W. Gao, C. Pan, J. K. Halsted, E. S. Chong, J. Lu, X. Wang, W. Luo, C.-H. Chang, Y. Wen, S. Ma, K. Amine and X. Ji, *Nano Energy*, 2015, **11**, 600.
31 J.-Z. Wang, L. Lu, M. Choucair, J. A. Stride, X. Xu and H.-K. Liu, *J. Power Sources*, 2011, **196**, 7030.
32 B. Wang, K. Li, D. Su, H. Ahn and G. Wang, *Chem.–Asian J.*, 2012, **7**, 1637.
33 Y. Yang, G. Yu, J. J. Cha, H. Wu, M. Vosgueritchian, Y. Yao, Z. Bao and Y. Cui, *ACS Nano*, 2011, **5**, 9187.
34 N. Li, M. Zheng, H. Lu, Z. Hu, C. Shen, X. Chang, G. Ji, J. Cao and Y. Shi, *Chem. Commun.*, 2012, **48**, 4106.
35 J. Yang, J. Xie, X. Zhou, Y. Zou, J. Tang, S. Wang, F. Chen and L. Wang, *J. Phys. Chem. C*, 2014, **118**, 1800.
36 C. Zu and A. Manthiram, *Adv. Energy Mater.*, 2013, **3**, 1008.
37 C. Wang, K. Su, W. Wan, H. Guo, H. Zhou, J. Chen, X. Zhang and Y. Huang, *J. Mater. Chem. A*, 2014, **2**, 5018.
38 B. Ding, C. Yuan, L. Shen, G. Xu, P. Nie, Q. Lai and X. Zhang, *J. Mater. Chem. A*, 2013, **1**, 1096.
39 S. Xin, L. Gu, N.-H. Zhao, Y.-X. Yin, L.-J. Zhou, Y.-G. Guo and L.-J. Wan, *J. Am. Chem. Soc.*, 2012, **134**, 18510.
40 H. B. Wu, S. Wei, L. Zhang, R. Xu, H. H. Hng and X. W. Lou, *Chem.–Eur. J.*, 2013, **19**, 10804.
41 H. Ye, Y.-X. Yin, S. Xin and Y.-G. Guo, *J. Mater. Chem. A*, 2013, **1**, 6602.
42 Y. Zhu, S. Murali, M. D. Stoller, K. J. Ganesh, W. Cai, P. J. Ferreira, A. Pirkle, R. M. Wallace, K. A. Cychosz, M. Thommes, D. Su, E. A. Stach and R. S. Ruoff, *Science*, 2011, **332**, 1537.
43 Y. Zhu, S. Murali, M. D. Stoller, A. Velamakanni, R. D. Piner and R. S. Ruoff, *Carbon*, 2010, **48**, 2118.
44 C. Zhang, H. B. Wu, C. Yuan, Z. Guo and X. W. Lou, *Angew. Chem., Int. Ed.*, 2012, **51**, 9592.
45 L. Yin, J. Wang, F. Lin, J. Yang and Y. Nuli, *Energy Environ. Sci.*, 2012, **5**, 6966.
46 Z. Li, L. Yuan, Z. Yi, Y. Sun, Y. Liu, Y. Jiang, Y. Shen, Y. Xin, Z. Zhang and Y. Huang, *Adv. Energy Mater.*, 2014, **4**, 1301473.
47 R. Elazari, G. Salitra, A. Garsuch, A. Panchenko and D. Aurbach, *Adv. Mater.*, 2011, **23**, 5641.
48 C.-P. Yang, Y.-X. Yin and Y.-G. Guo, *J. Phys. Chem. Lett.*, 2015, **6**, 256.

